A Novel Computerized Tool to Stratify Risk in Carotid Atherosclerosis Using Kinematic Features of the Arterial Wall

Aimilia Gastounioti, *Member, IEEE*, Stavros Makrodimitris, Spyretta Golemati, *Member, IEEE*, Nikolaos P. E. Kadoglou, Christos D. Liapis, and Konstantina S. Nikita, *Senior Member, IEEE*

***Abstract*—Valid characterization of carotid atherosclerosis (CA) is a crucial public health issue, which would limit the major risks held by CA for both patient safety and state economies. This paper investigated the unexplored potential of kinematic features in assisting the diagnostic decision for CA in the framework of a computer-aided diagnosis (CAD) tool. To this end, 15 CAD schemes were designed and were fed with a wide variety of kinematic features of the atherosclerotic plaque and the arterial wall adjacent to the plaque for 56 patients from two different hospitals. The CAD schemes were benchmarked in terms of their ability to discriminate between symptomatic and asymptomatic patients and the combination of the Fisher discriminant ratio, as a feature-selection strategy, and support vector machines, in the classification module, was revealed as the optimal motion-based CAD tool. The particular CAD tool was evaluated with several cross-validation strategies and yielded higher than 88% classification accuracy; the texture-based CAD performance in the same dataset was 80%. The incorporation of kinematic features of the arterial wall in CAD seems to have a particularly favorable impact on the performance of image-data-driven diagnosis for CA, which remains to be further elucidated in future prospective studies on large datasets.**

***Index Terms*—Carotid atherosclerosis (CA), computer-aided diagnosis (CAD), kinematic features, motion analysis, ultrasound (US).**

I. Introduction

CAROTID atherosclerosis (CA) is a chronic degenerative disease, gradually resulting in the formation of lesions (plaques) in the inner lining of the carotid artery. Atherosclerotic plaques may lead to severe narrowing of the arterial lumen with detrimental impact on blood supply and major risks for cerebrovascular disorders; it is well established that CA highly predisposes to cerebral ischemic events, with the majority of stroke events being provoked due to the disease [1]. The high morbidity, disability, and mortality rates associated with stroke in Europe [2] and in the United States [3], in combination with the negative predictions for the future based on the current secular trends [4], pose a major need for valid risk assessment and optimal treatment selection (carotid revascularization or conservative therapy with medication and dietary) for patients with CA.

In current clinical practice, the therapeutic decision for patients with asymptomatic CA (i.e., with no history of CA-induced neurological disorders) relies on the ultrasonographically measured degree of lumen stenosis [5]. However, there is evidence that this marker is not sufficient [6], thereby motivating the development of computer-aided-diagnosis (CAD) systems, which incorporate additional markers to assist treatment planning. In particular, the development of CAD systems which are based on 2-D ultrasound (US) image analysis is considered as a grand challenge by the scientific community, because 1) traditionally, vascular physicians select US examination in diagnosis and follow-up for patients with CA, 2) the use of affordable imaging techniques, such as US, is crucial to avoid increasing the socioeconomic burden of the disease, and 3) 2-D US is traditionally available on commercial US systems [7], [8].

A typical CAD tool consists of two main modules, namely the feature-selection module, which spares the most clinically useful features from redundant ones, and the classifier, which is trained, using the selected subset of features. Advanced methods of image processing allow the extraction of a large number of features, which may be difficult to interpret and to classify. Therefore, feature selection is a crucial step in the CAD design to simplify both the feature vector and the classifier. It is also very important to enhance the computational performance of the CAD system in terms of execution time and memory requirements.

Table I summarizes key studies in the particular research area [9]–[17], which are based on the analysis of B-mode US, i.e., the typical 2-D US imaging modality for the carotid artery wall. In all cases, the underlying idea was computer-assisted discrimination of high-risk atherosclerotic lesions from low-risk ones, by estimating image-based features of symptomatic and asymptomatic patients with CA and using the estimated features to train appropriately designed CAD tools.

Manuscript received December 24, 2013; revised March 31, 2014; accepted May 29, 2014. Date of publication June 9, 2014; date of current version May 7, 2015. This work was supported in part by the Operational Program "Competitiveness and Entrepreneurship" and Regional Operational Programmes of the National Strategic Reference Framework 2007–2013 and "SYNERGASIA": "Collaborative projects of small and medium scale." The work of A. Gastounioti was supported in part by a scholarship from the Hellenic State Scholarships Foundation.

A. Gastounioti, S. Makrodimitris, and K. S. Nikita are with the School of Electrical and Computer Engineering, National Technical University of Athens, Athens 10682, Greece (e-mail: gaimilia@biosim.ntua.gr, stamakro@gmail.com, knikita@ece.ntua.gr).

S. Golemati is with the First Intensive Care Unit, Medical School, National Kapodistrian University of Athens, Athens 10679, Greece (e-mail: sgolemati@med.uoa.gr).

N. P. E. Kadoglou and C. D. Liapis are with the Attikon University General Hospital, National Kapodistrian University of Athens, Athens 10679, Greece (e-mail: nkado@med.uoa.gr, liapis@med.uoa.gr).

Color versions of one or more of the figures in this paper are available online at http://ieeexplore.ieee.org.

Digital Object Identifier 10.1109/JBHI.2014.2329604

TABLE I
KEY STUDIES ON DEVELOPING COMPUTER-AIDED DIAGNOSTIC TOOLS, WHICH ARE BASED ON B-MODE US IMAGE ANALYSIS TO STRATIFY RISK IN ATHEROSCLEROTIC CAROTID ARTERIES

Study / year		Classifiers	Feature selection	Maximum accuracy
[9]	2003	SOM, kNN	ST	73.1%
[11]	2007	NN	ST	99.1%
[12]	2007	SVM, PNN	PCA	73.4%
[13]	2009	SVM, PNN	PCA	73.7%
[10]	2011	SVM, PNN	ST	85%
[14]	2012	SVM, kNN, PNN, DT	ST	89.5%
[15]	2012	SVM	ST	79.3%
[16]	2012	SVM	ST	83.7%
[17]	2013	SVM	ST	91.7%

SOM: self-organizing maps; kNN: k-nearest neighbor; SVM: support vector machines; NN: neural network; PNN: probabilistic neural network; DT: decision trees; ST: statistical tests; PCA: principal component analysis.

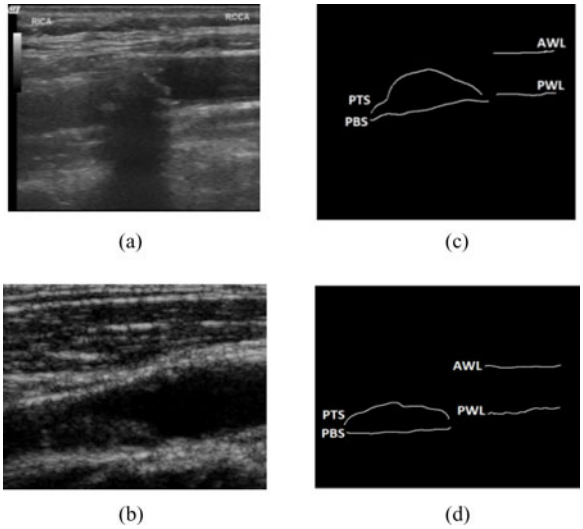

Fig. 1. Examples of (a), (b) B-mode US images of the carotid artery, and (c), (d) the selected ROIs for patients from (a), (c) the Attikon University Hospital of Greece and (b), (d) the St. Mary's Hospital of UK.

In most studies, feature selection was based on statistical tests, while a few ones used principal component analysis (PCA) to remove redundant features [12], [13]. Multiple classifiers, such as self-organizing maps [9], support vector machines (SVM) [10], [12]–[17], k-nearest neighbor (kNN) [9], [14], decision trees (DT) [14], neural networks [11], and probabilistic neural networks (PNN) [10], [12]–[14], were used, with SVM, PNN, and kNN being most popular in the field. Moreover, DT and discriminant analysis (DA) have been successfully used in CAD tools for other vascular disorders involving the coronary artery [18] and the pulmonary vessel tree [19], respectively.

Regarding image-based features, plaque texture has been thoroughly investigated, with very encouraging results by CAD tools [7]. The morphology of the arterial wall has also been included in a limited number of CAD systems, without gaining as much attention [7]. The role of kinematic features, which are estimated with motion analysis from B-mode US image sequences and represent dynamic phenomena and mechanical interactions occurring during the cardiac cycle (CC), remains unexplored, though. None of the related studies has considered kinematic features in CAD systems for CA, while only a few research groups have investigated potential motion-based risk markers [20], [21].

Based on the above, the objective of this study is to elucidate the role of kinematic features of the arterial wall in computer-assisted risk stratification in CA by identifying an optimal motion-based CAD tool for the disease. To this end, 15 CAD schemes are designed by combining three feature-selection methods with five classifiers; specifically, two statistical methods, namely the Fisher discriminant ratio (FDR) and the Wilcoxon rank-sum test (WRS), and PCA are used for feature selection, while SVM, kNN, PNN, DT, and DA are used in the classification module. Subsequently, kinematic features of the atherosclerotic plaques and normal parts of the arterial wall adjacent to the plaques are estimated for 56 symptomatic and asymptomatic patients with CA from two different hospitals. The designed CAD schemes are, then, fed with the estimated kinematic features, they are optimized in terms of their design parameters, and they are benchmarked in terms of their ability to discriminate between symptomatic and asymptomatic cases. Finally, the optimal CAD scheme is also benchmarked against texture-based classification in the same dataset.

II. MATERIAL AND METHODS

A. US Image Data: Acquisition and Preprocessing

A total of 56 elderly patients (aged 50–90) with established CA (diagnosed carotid stenosis >50%), who were referred to the St. Mary's Hospital of U.K. ($N = 28$) [21] and the Attikon General University Hospital of Greece ($N = 28$) [22] for carotid artery US scanning, were selected. Among those patients, 28 (St. Mary's: 18, Attikon: 10) had experienced an ischemic cerebrovascular event, i.e., stroke or transient ischemic attack ("symptomatic" group), while 28 patients (St. Mary's: 10, Attikon: 18) had no neurological symptoms ("asymptomatic" group), within a 6-month time period before the time of examination. No statistically significant differences were found in the ages or in the degrees of stenosis between patient subgroups ("symptomatic" and "asymptomatic" or "St. Mary's" and "Attikon"). The differences in US image recordings of the two hospitals, in terms of US equipment and operator, form a challenging dataset, which constitutes a key feature of this study.

The local institutional review boards approved US image examinations and all subjects gave their informed consent to the scientific use of the data. For each subject, the carotid artery was scanned in the longitudinal direction according to a standardized protocol (dynamic range, 60 dB; persistence, low) and a B-mode US image sequence was recorded at a rate higher than 25 frames/s for at least 3 s (2–3 consecutive CCs). Dynamic B-mode US imaging of longitudinal sections of the arterial wall allows the estimation of tissue motion in two dimensions, namely longitudinal, i.e., along the vessel axis, and radial, i.e., along the vessel radius, and perpendicular to the longitudinal

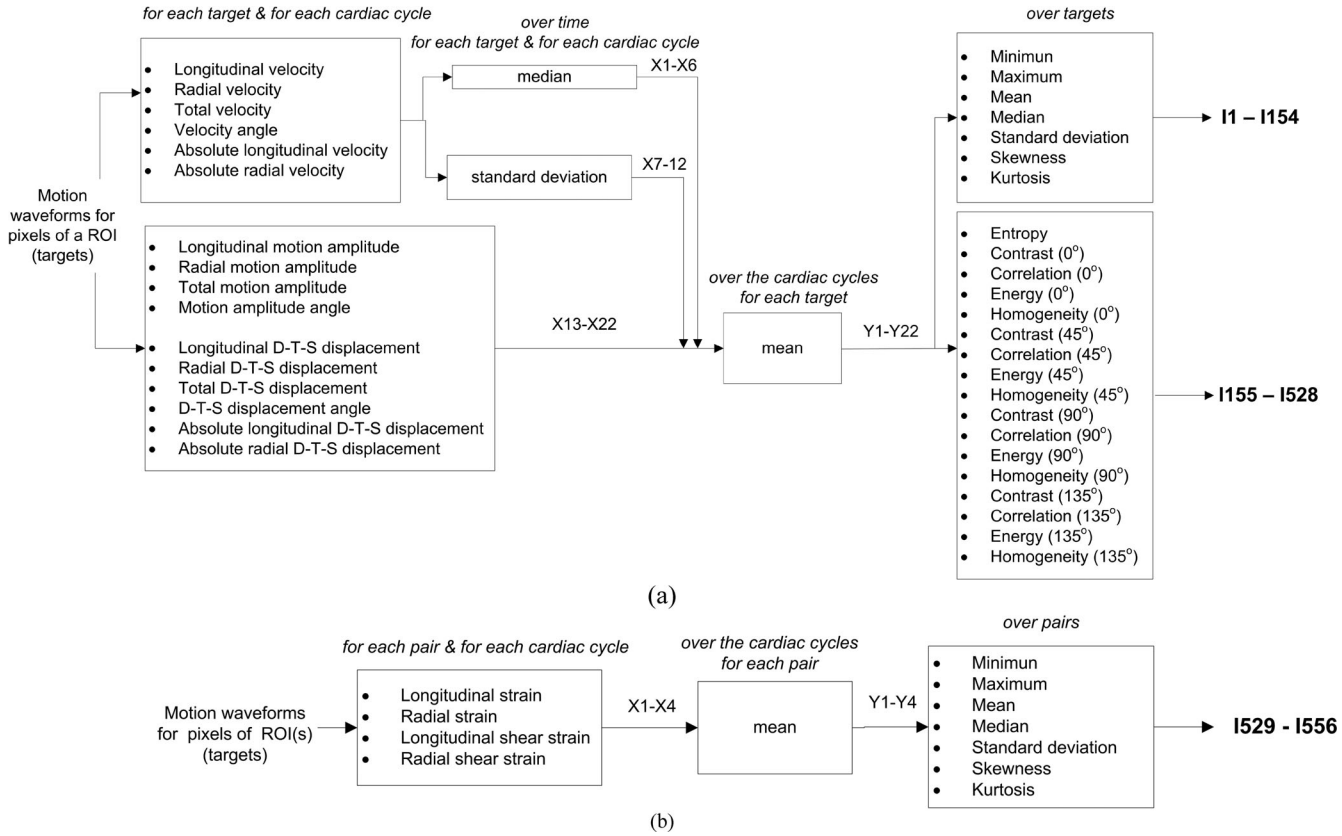

Fig. 2. Schematic presentation of the steps followed to estimate statistical measures of (a) pixel-wise kinematic and (b) pair-wise strain indices, using the results of motion analysis for a ROI or a pair of ROIs. D-T-S: diastole-to-systole.

one. Fig. 1(a) and (b) shows examples of B-mode US image recordings for patients with atherosclerotic plaques at the posterior arterial wall.

For each clinical case, an experienced vascular physician traced four regions of interest (ROIs), namely the posterior (PWL) and anterior wall-lumen (AWL) interfaces, and the plaque top (PTS) and bottom surfaces (PBS) [see Fig. 1(c) and (d)]. PWL and AWL are normal parts of the arterial wall adjacent to the plaques and they were included in motion analysis, because recent studies have revealed US image-based features of healthy parts of the arterial wall close to the plaque as potential risk markers for CA [21], [23]. Subsequently, image intensities ([0: black, 255: white]) were linearly adjusted so that the median grey level value of the blood was 0, and the median grey level value of the adventitia was 190 [24]. This preprocessing step was necessary to ensure comparable measurements between the two subsets of image recordings.

B. Feature Extraction

All pixels composing the four ROIs, as well as the whole plaque region (i.e., the region contoured by PTS and PBS), were selected as motion targets. The radial and longitudinal positions of the targets across time were estimated using $\mathrm{ABM}_{\mathrm{KF-K2}}$, a recently proposed motion estimator with enhanced accuracy in motion tracking of the arterial wall from both artifacts-free and artifacts-corrupted image recordings [21], [25].

From the produced waveforms, a wide variety of kinematic and strain indices can be estimated (see Fig. 2). Specifically, kinematic indices can be produced by estimating target-wise indices representing 1) median and standard deviation in velocities during the CC, 2) motion amplitudes, defined as the absolute difference between the corresponding maximum and minimum target positions, and 3) diastole-to-systole displacements, for each CC [see Fig. 2(a)]. Strain indices can be estimated, using motion waveforms for pairs of pixels [Fig. 2(b)] and they express relative movements between ROIs or local deformations in an ROI during the CC [21], [26]. In all cases, descriptive statistical measures of the mean (over the CCs) values of the target- or pair-wise indices are calculated.

In this study, 1144 kinematic indices for PWL, AWL, PTS, PBS, and the plaque region were estimated. Moreover, 93 strain indices were used to express relative movements between 1) PWL and AWL, 2) PTS and PBS, 3) PTS and PWL or AWL, and 4) PBS and PWL or AWL (if the plaque was located at the posterior or the anterior wall, respectively), and local deformations in PWL, AWL, and PTS. As a result, a total number of 1236 kinematic features were produced for each patient. Table II defines the aforementioned features, following the index encoding of Fig. 2.

For direct comparisons of the CAD performance in the same study group, using either kinematic or textural features, plaque texture was measured by applying a multiresolution approach for image analysis, which is based on wavelet packets [10].

TABLE II
KINEMATIC FEATURES WHICH WERE ESTIMATED FOR EACH PATIENT, USING THE PRODUCED MOTION WAVEFORMS OF THE TARGETS OF A ROI OR A PAIR OF ROIS

ROI(s)	Index encoding of Fig. 2	Kinematic features
Kinematic indices		
PWL	I1–I154	F1–F154
AWL	I1–I154	F155–F308
PTS	I1–I154	F309–F462
PBS	I1–I154	F463–F616
plaque region	I1–I528	F617–F1144
Strain indices		
PWL	I529–I535	F1145–F1159
	I550–I556	
AWL	I529–I535	F1160–F1173
	I549–I556	
PWL, AWL	I536–I542	F1174–F1180
PTS	I529–I535	F1181–F1194
	I550–I556	
PTS, PBS	I536–I549	F1195–F1208
PTS, PWL, or AWL	I529–I542	F1209–F1222
PBS, PWL, or AWL	I529–I542	F1223–F1236

ROI: region of interest; PWL: posterior wall-lumen, AWL: anterior wall-lumen; PTS: plaque top surface; PBS: plaque bottom surface.

Briefly, for each patient, systolic and diastolic images were decomposed up to three levels using the wavelet packets, leading to 126 detail subimages. Then, the mean and standard deviation of image intensities of the produced subimages were estimated, resulting in a total number of 252 textural features. This approach was selected among other textural measures, considering that wavelet-based image decomposition is a state-of-the-art methodology in the area of texture analysis and it has been used in the latest studies on texture classification of atherosclerotic tissue from B-mode US images [10], [14]–[17].

C. Design of CAD Schemes

In this study, 15 CAD schemes were designed, based on combinations between three feature-selection methods (FDR, WRS, and PCA) and five classifiers (SVM, PNN, kNN, DT, and DA). In the following, the main underlying principles and the corresponding parameterization (based on previous experience in the particular research area [9]–[19]) of these modules are briefly described.

Feature selection aims at the identification of those features, which are able to better separate the "symptomatic" and "asymptomatic" groups. In FDR and WRS, a feature is considered to have a strong discrimination power, if it corresponds to a high FDR value and a low p-value, respectively. Therefore, features are sorted in descending FDR value or ascending p-value, and an optimal feature subset is a set of m features, consisting of the 1st, 2nd, ..., mth features. In PCA, the set of features is converted into a reduced number of uncorrelated features (principal components), while retaining most of its information content. This transformation is defined in such a way that the first principal component has the largest possible variance, i.e., it accounts for as much of the variability in the data as possible, while components having variance less than a threshold (*thr*) are removed. The design parameter of both FDR and WRS is m (in [1–100]), while PCA is affected by *thr* (in [0.0001–0.1]).

SVM are learning machines based on intuitive geometric principles, aiming to the definition of an optimal hyper plane, which separates the training data so that a minimum expected risk is achieved [27]. Compared to other classifiers, SVM is less affected by the so-called "curse of dimensionality" and is therefore suitable for large sets of features [28]. The training method is based on a nonlinear mapping of the dataset, using kernels that have to satisfy Mercer's theorem. In this study, a Gaussian radial basis function (RBF) kernel was used. In this case, the SVM training algorithm is affected by the parameter s (in [0.5–10]), defining the spread of RBF, which has to be appropriately adjusted to optimize the performance of the classifier.

The PNN is a multilayered feedforward neural network, which is faster, more accurate, and less sensitive to outliers than multilayer perceptron networks [29]. The first layer (input layer) computes distances from the input vector to the training input vectors and produces a vector whose elements indicate how close the input is to a training input. The second layer (radial basis layer) takes into account the classes to which the training examples belong to and produces a vector of probabilities for the input vector. In this layer, an RBF is applied to each distance to compute the influence for each training vector. Finally, a competitive output layer picks the maximum of these probabilities and classifies the input vector to the corresponding class. In this study, a Gaussian RBF was used and the design parameter of PNN was s (in [0.5–10]). kNN is conceptually similar to PNN; kNN is a simple classifier, in which a feature vector is assigned the class that is most common among its k nearest neighbors, based on some similarity measure (distance function) [30]. The classification performance of kNN depends on the parameter k (in [3–11]) and the distance function (in {city block, Chebyshev, standardized Euclidean, cosine, Euclidean, Hamming, Jaccard, Minkowski}).

A DT consists of internal nodes (i.e., nodes with outgoing edges) and leaves (or decision nodes) that form a rooted tree. Each internal node splits the instance space into two or more subspaces and each path from the root to a leaf is transformed into a rule by conjoining the tests along the path to form the antecedent part and taking the leaf's class as the class prediction. Therefore, in a DT classifier, a set of rules for the different classes is derived from input features of the training data and is then used to classify a new input vector [31]. For optimal performance of the DT, the most suitable split criterion (in {Gini, twoing, deviance}) and the transformation function (*tf*) for the posterior probabilities (scores) should be defined. In this study, the following *tf*s were investigated for scores x: $\{x, 2x-1, \log(x/(1-x))$, "set score for the class with the largest score to 1, and scores for all other classes to 0," "set score for the class with the largest score to 1, and scores for all other classes to -1", $1/(1+e^{\wedge}(-x)), 1/(1+e^{\wedge}(-2x)), 2/(1+e^{\wedge}(-x))-1$, sign of $x\}$.

DA is a classification method, which assumes that different classes generate data based on different Gaussian distributions. The DA classifier is trained with a fitting function, which estimates the parameters of a Gaussian distribution for each class,

while a new vector is classified by finding the class with the lowest misclassification cost. In DA, the only parameter which needs to be defined is the type of DA, i.e., linear, quadratic, diagonal linear, or diagonal quadratic DA [32].

D. Optimization and Benchmarking

The designed CAD schemes were implemented in MATLAB (The MathWorks, Natick, MA, USA), using the Bioinformatics and the Statistics Toolboxes. Subsequently, they were fed with the set of kinematic features, i.e., vectors of 1236 motion-based indices for 56 patients, and were optimized in terms of the corresponding design parameterization, i.e., the parameters of both the feature-selection and the classification modules. The optimization step was necessary to reveal the full potential of motion-based CAD schemes. The CAD performance was measured in terms of classification accuracy, i.e., percentage of correctly classified cases, using leave-one-out cross validation. In leave-one-out, a single observation (patient) is used as the testing sample, and the remaining observations compose the training dataset; this is repeated such that each observation is used once as the testing sample. Leave-one-out is a popular resampling technique for performance evaluation for classification schemes, because it preserves unbiased results for small-sized samples [33].

The potential of the optimal motion-based CAD scheme was further validated with the following two-step process. First, the corresponding CAD performance was compared with the optimal performance, which can be achieved by a texture-based CAD scheme in the same dataset. To this end, the designed CAD schemes were fed with vectors of 252 textural features for 56 patients and the optimal texture-based CAD scheme was identified with the same aforementioned optimization process.

In a second step, the performance of the optimal motion-based CAD scheme was measured using eight different cross-validation strategies, namely tenfold, hold-out, repeated random subsampling with either overlapping (resub1) or nonoverlapping (resub2) training and testing sets in both stratified and nonstratified versions [33]. Stratified strategies produce more valid conclusions on the generalization performance of the classifier than nonstratified ones, because stratification assures that the training dataset is reasonably representative. In this step, the CAD performance was measured in terms of classification accuracy, sensitivity (percentage of correctly classified symptomatic patients as symptomatic), and specificity (percentage of correctly classified asymptomatic patients as asymptomatic). The area under the receiver operating characteristic (ROC) curve was also used to measure the CAD performance; the ROC curve describes the inherent discrimination capacity of the CAD scheme and the area under the ROC curve (auc) ranges from 0.5 (random discriminatory accuracy, which represent no realistic classifier) to 1.0 (perfect discriminatory accuracy) [34].

III. Results

Table III presents the classification accuracy that was achieved by each motion-based CAD scheme after having been optimized. FDR generally yielded higher accuracy values than other feature-selection methodologies, while SVM and kNN were the most effective classifiers. These CAD components were also computationally efficient (see Fig. 3). Highest classification accuracy (88%) was achieved by the combination of FDR (with $m = 23$) with an SVM classifier (with $s = 5.73$). In an attempt to also assess the computational cost in cases of medium- and large-scale clinical studies, the CAD components were applied to synthetic datasets consisting of 1236 motion-based indices for 50–300 patients. According to the results (see Fig. 3), the presented CAD schemes would be sufficiently efficient in such cases.

Table IV presents similar results for texture-based CAD schemes. In this case, the DT classifier yielded higher classification performances than other classifiers, while the WRS was the most effective feature-selection methodology. The optimal performance (80%) was achieved by the combination of the PCA (with $thr = 0.017$) with the DT classifier (with Gini as split criterion and *tf* = "set score for the class with the largest score to 1, and scores for all other classes to 0").

TABLE III
CLASSIFICATION ACCURACY OF 15 OPTIMIZED CAD SCHEMES, GENERATED BY COMBINING THREE FEATURE-SELECTION METHODS WITH FIVE CLASSIFIERS, USING KINEMATIC FEATURES OF THE ARTERIAL WALL

Classifier Feature selection	SVM	PNN	kNN	DT	DA
FDR	**0.88**	0.75	0.82	0.75	0.71
WRS	0.80	0.64	0.75	0.68	0.68
PCA	0.70	0.57	0.73	0.80	0.77

Boldface indicates maximum accuracy.

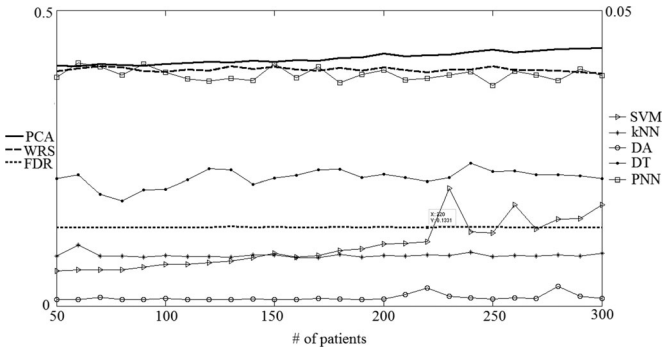

Fig. 3. Computing time, in *s*, of three feature selection methods (left axis) and five classifiers (right axis) for different dataset sizes (i.e., # of patients).

TABLE IV
CLASSIFICATION ACCURACY OF 15 OPTIMIZED CAD SCHEMES, GENERATED BY COMBINING THREE FEATURE-SELECTION METHODS WITH FIVE CLASSIFIERS, USING TEXTURAL FEATURES OF THE ARTERIAL WALL

Classifier Feature selection	SVM	PNN	kNN	DT	DA
FDR	0.66	0.63	0.70	0.73	0.68
WRS	0.71	0.64	0.71	0.71	0.71
PCA	0.63	0.57	0.66	**0.80**	0.64

Boldface indicates maximum accuracy.

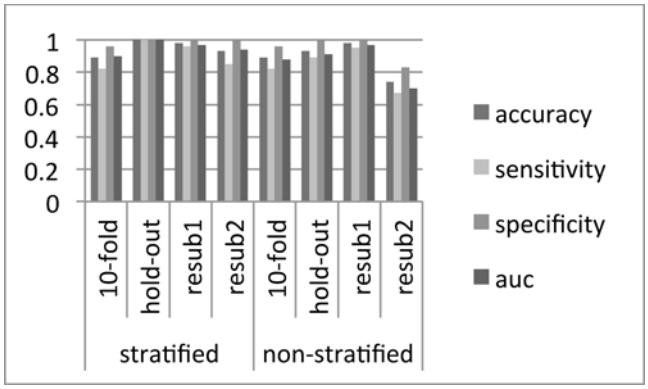

Fig. 4. Bar charts for the classification accuracy, sensitivity, specificity, and auc, when eight different stratified or nonstratified cross-validation strategies were applied to the optimal motion-based CAD scheme.

Based on the comparison of Tables III and IV, it was concluded that the incorporation of kinematic features in CAD was superior to texture-based CAD, in terms of classification performance. The bar charts of Fig. 4 summarize the results from the CAD performance evaluation of the optimal motion-based CAD scheme, using eight different cross-validation techniques. In all cases, accuracy, sensitivity, specificity, and auc were higher than 0.74, 0.67, 0.83, and 0.70, respectively. However, if only the stratified cross-validation methods are considered, the minimum accuracy, sensitivity, specificity, and AUC values were higher (0.88, 0.82, 0.96, and 0.90, respectively). At this point, it is also worth mentioning that the optimal motion-based CAD scheme reached classification accuracy of 96%, when it was applied separately to the patients of each hospital.

Table V lists the 23 kinematic features, which are used in the optimal motion-based CAD scheme. For each feature, the index (according to the encoding of Table II), a short description, the mean values in the two patient groups (i.e., symptomatic and asymptomatic groups), and the FDR between the two patient groups are presented. Considering the descriptions of the features, this CAD scheme incorporates kinematic indices, which represent motion properties of AWL, PTS, and the whole plaque region, as well as strain indices, which express local deformations in PWL and the relative longitudinal movement between PTS and the healthy part of the wall adjacent to the plaque (PWL or AWL). Generally, compared with asymptomatic patients, symptomatic ones were found to have higher radial and lower longitudinal movements of AWL. Moreover, the same patient group displayed higher inhomogeneity in radial and longitudinal movements within PTS; the same was observed for radial and longitudinal movements within the plaque region. In addition, it was found that, in symptomatic patients, local deformations in the longitudinal direction both between different regions of PWL and between PTS and PWL/AWL increased with respect to asymptomatic subjects.

IV. Discussion

Valid risk stratification in CA is a crucial public health issue toward enhanced patient safety and low socioeconomic burden of the disease. Motivated by recent findings, which suggested that motion-based markers are able to contribute to objective characterization of atherosclerotic plaques in the carotid artery [21], this study went one step further by thoroughly investigating that the CAD scheme which reveals the full potential of motion analysis in risk stratification in CA. The novelty of this work lies not only in the incorporation of motion analysis in CAD tools for CA, which has not been attempted in related published work (see Table I), but also in the framework which was used to identify and evaluate the optimal motion-based CAD scheme.

The special features of this framework, which are hereafter described, enhance validity and they limit bias in the generated conclusions on the CAD performance. First, a medium-sized, yet carefully designed, balanced, and challenging, dataset was used; the study group consisted of two equal-sized subsets of patients from two different hospitals. Moreover, a wide variety of kinematic features of the plaque and healthy parts of the arterial wall adjacent to plaque were investigated. In addition, in an attempt to consider intra-ROI variability of motion properties and to avoid invalid results due to outliers, motion-based measurements were repeated for multiple targets, or pairs of targets, of the selected ROIs. From the CAD aspect, the optimal CAD scheme was selected among 15 alternatives, which were first systematically optimized for the particular clinical application in terms of their design parameterization. The most effective CAD tool was further evaluated using several cross-validation techniques, which are suitable for relatively small datasets. Finally, to provide objective comparisons with state-of-the-art work in the field, the optimal motion-based CAD scheme was benchmarked against the texture-based CAD performance.

Among 15 candidate CAD schemes, a combination of the SVM classifier and the FDR feature-selection tool was revealed as the optimal choice for motion-based plaque classification. In this case, classification accuracy reached 88%, which was maintained in all the evaluation tests using different stratified cross-validation strategies (see Fig. 4). The same CAD scheme achieved 96% classification accuracy when applied separately to the patient data of each hospital. This is considered a reasonable finding, as US examination by the same operator using the same US equipment reduces heterogeneity in image recordings for cases with similar kinematic features of the arterial wall; in this case, motion analysis, which is affected by US image quality [21], [25], reveals potential differences between subgroups of patients even on relatively small datasets. However, larger datasets may be necessary to maximize the CAD performance and maintain high classification accuracy for multisource image recordings.

Based on the above, and considering that none of the related studies (see Table I) has tested CAD schemes on multisource image recordings, direct comparisons can be performed only for the single-source CAD performance (96%). These comparisons place the proposed CAD scheme among the most effective ones, while the multisource CAD performance (88%) also falls within the range of previously published results, thereby revealing the potential of motion analysis in the field. This conclusion is further reinforced if we consider that the particular CAD scheme

TABLE V
LIST OF KINEMATIC FEATURES WHICH ARE INCORPORATED IN THE OPTIMAL MOTION-BASED CAD SCHEME

Index	Description	S	AS	FDR	Index	Description	S	AS	FDR
over targets of AWL									
F163	Maximum of median radial velocity	0.222	0.102	0.244	F197	Minimum of std of longitudinal velocity	0.303	0.421	0.188
F165	Median of median radial velocity	0.114	0.025	0.347	F214	Median of std of radial velocity	0.111	0.027	0.312
F176	Minimum of median velocity angle	−0.367	−0.172	0.276	F289	Maximum of D-T-S displacement angle	0.926	0.675	0.192
F181	Skewness of median velocity angle	–0.036	0.265	0.177	F295	Minimum of absolute longitudinal D-T-S displacement	0.033	0.059	0.270
over targets of PTS									
F406	Kurtosis of radial motion amplitude	3.259	2.751	0.205	F426	Skewness of longitudinal motion amplitude	0.567	0.185	0.187
F413	Kurtosis of total motion amplitude	3.336	2.719	0.228	F461	Skewness of absolute radial D-T-S displacement	0.771	0.470	0.175
F419	Skewness of amplitude angle	0.266	0.604	0.192	F462	Kurtosis of absolute D-T-S radial displacement	3.519	2.746	0.240
over targets of plaque region									
F665	Kurtosis of std of longitudinal velocity	3.954	3.230	0.195	F1062	Correlation (0°) of radial D-T-S displacement	0.898	0.912	0.192
F749	Kurtosis of total D-T-S displacement	3.762	2.782	0.283	F1070	Correlation (90°) of radial D-T-S displacement	0.831	0.842	0.186
F793	Kurtosis of absolute D-T-S longitudinal displacement	4.093	3.148	0.247	F1074	Correlation (135°) of radial D-T-S displacement	0.817	0.820.	0.195
over pairs of targets of PWL									
F1151	Kurtosis of LSI	12.710	21.141	0.223	F1150	Skewness of LSI	–2.043	–3.519	0.236
over pairs of targets of PTS and PWL/AWL									
F1214	Skewness of LSI	2.541	1.442	0.287					

For Each Feature, the Index (according to the encoding of Table II), a Short Description, the Mean Values for Symptomatic (S) and Asymptomatic (AS) Patients, and the Fisher Discriminant Ratio (FDR) Between the Two Groups of Patients are Presented.
std: standard deviation; D-T-S: diastole-to-systole; PWL: posterior wall-lumen, AWL: anterior wall-lumen; PTS: plaque top surface; LSI: longitudinal strain.

also outperformed the texture-based CAD performance in the same dataset.

With SVM having been particularly popular in studies toward US-image-based characterization of atherosclerotic plaques, the results of Table III confirmed the suitability of this classifier to the development of CAD tools for CA. However, it is worth mentioning that, for textural features, the CAD performance was maximized by a CAD scheme which relied on the combination of the DT classifier with PCA. Given that DT [14] and PCA [12], [13] have been used in a limited number of texture-based CAD tools for CA and their combination has not been investigated, this finding would be very useful in the design of future studies on texture-based classification of atherosclerotic plaques.

The optimal motion-based CAD scheme incorporates 23 kinematic and strain features which are related with motion properties of AWL, PWL, PTS, and the whole plaque region, as well as relative movements between PTS and the healthy part of the wall adjacent to the plaque. Although different indices were identified as potential risk markers in the latest authors' works where only the patients from the St. Mary's [21] or the Attikon hospital were considered [22]; all studies revealed that the mobility features of the atherosclerotic lesion itself and healthy parts of the wall close to the lesion are equally important in risk stratification in the disease. Based on these results, plaque vulnerability seems to be significantly affected by dynamic phenomena which occur in a wide region around the atherosclerotic lesion. In this study, these dynamic phenomena were captured in 2-D motion analysis. Although it has been recently suggested that 2-D motion carries sufficient information for characterizing the arterial wall [21], [22], [35], investigating the CAD contribution of out-of-plane motion constitutes an interesting future perspective.

The performance of the proposed motion-based CAD scheme provides an encouraging feedback on the role of kinematic features of the arterial wall in the therapeutic decision for CA and it is expected to motivate the incorporation of motion analysis in future-related studies designing CAD tools for the disease. Inspired by recent studies on cerebral aneurysms [36], [37], it would also be interesting to combine image-based motion analysis with computational fluid dynamics in an attempt to gain insight in the biomechanical behavior of vulnerable atherosclerotic lesions. Kinematic features seem to have the potential to contribute to valid clinical assessment of the disease phenotype, which remains to be proved by future retrospective and prospective studies on enriched datasets with frequent patient follow-ups.

V. CONCLUSION

This study revealed the potential of motion analysis in risk stratification in CA, by proposing a novel CAD scheme, which is based on kinematic features to assist the identification of vulnerable atherosclerotic lesions. The proposed CAD scheme is a combination of an FDR feature-selection module with an SVM classifier and it achieved 88% classification accuracy in a challenging dataset consisting of patients from two different hospitals. The motion-based CAD performance was thoroughly evaluated using multiple cross-validation techniques and it was also found to be superior to texture-based characterization of

atherosclerotic plaques in the same dataset. Based on the above, motion analysis seems to have a valuable role in the field of image-driven CAD for CA and should be included in future attempts toward personalized and objective diagnosis for the disease.

ACKNOWLEDGMENT

The authors would like to thank the expert clinicians of the Irvine Laboratory, St. Mary's Hospital of U.K. (Prof. A. N. Nicolaides), and Dr. C. Gkekas, Dr. J. D. Kakisis, and Dr. A. Koulia from the Department of Vascular Surgery, Attikon University General Hospital of Greece for their valuable contribution in collecting the US image data. The authors would also like to thank N. Tsiaparas for his help on texture analysis.

REFERENCES

[1] D. R. Labarthe, *Epidemiology and Prevention Of Cardiovascular Diseases: A Global Challenge*. Boston, MA, USA: Jones & Bartlett Learning, 2011.

[2] M. Nichols, N. Townsend, R. Luengo-Fernandez, J. Leal, P. Scarborough, and M. Rayner, "European cardiovascular disease statistics (2012)," *Eur. Heart Netw. Eur. Soc. Cardiol.*, Brussels, European Society of Cardiology, Sophia Antipolis. Available: http://www.escardio.org/about/Documents/EU-cardiovascular-disease-statistics-2012.pdf

[3] V. L. Roger, A. S. Go, D. M. Lloyd-Jones, E. J. Benjamin, J. D. Berry, W. B. Borden, D. M. Bravata, S. Dai, E. S. Ford, C. S. Fox, H. J. Fullerton, C. Gillespie, S. M. Hailpern, J. A. Heit, V. J. Howard, B. M. Kissela, S. J. Kittner, D. T. Lackland, J. H. Lichtman, L. D. Lisabeth, D. M. Makus, G. M. Marcus, A. Marelli, D. B. Matchar, C. S. Moy, D. Mozaffarian, M. E. Mussolino, G. Nichol, N. P. Paynter, E. Z. Soliman, P. D. Sorlie, N. Sotoodehnia, T. N. Turan, S. S. Virani, N. D. Wong, D. Woo, and M. B. Turner, "Heart disease and stroke statistics—2012 update. A report from the American Heart Association," *Circulation*, vol. 125, no. 1, pp. e2–e220, 2012.

[4] C. D. Mathers and D. Loncar, "Projections of global mortality and burden of disease from 2002 to 2030," *PLoS Med.*, vol. 3, no. 11, p. e442, 2006. Available: http://www.ncbi.nlm.nih.gov/pubmed/17132052

[5] M. Tendera, V. Aboyans, M. L. Bartelink, I. Baumgartner, D. Clément, J. P. Collet, A. Cremonesi, M. De Carlo, R. Erbel, F. G. Fowkes, M. Heras, S. Kownator, E. Minar, J. Ostergren, D. Poldermans, V. Riambau, M. Roffi, J. Röther, H. Sievert, M. van Sambeek, and T. Zeller, "ESC Guidelines on the diagnosis and treatment of peripheral artery diseases: Document covering atherosclerotic disease of extracranial carotid and vertebral, mesenteric, renal, upper and lower extremity arteries: The task force on the diagnosis and treatment of peripheral artery diseases of the European Society of Cardiology," *Eur. Heart J.*, vol. 32, no. 22, pp. 2851–2906, 2011.

[6] A. R. Naylor, "Time to rethink management strategies in asymptomatic carotid artery disease," *Nature Rev. Cardiol.*, vol. 9, no. 2, pp. 116–124, 2011.

[7] S. Golemati, A. Gastounioti, and K. S. Nikita, "Toward novel noninvasive and low-cost markers for predicting strokes in asymptomatic carotid atherosclerosis: The role of ultrasound image analysis," *IEEE Trans. Biomed. Eng.*, vol. 60, no. 3, pp. 652–658, Mar. 2013.

[8] K. S. Nikita, "Atherosclerosis: The evolving role of vascular image analysis," *Comput. Med. Imag. Graph.*, vol. 37, no. 1, pp. 1–3, 2013.

[9] C. I. Christodoulou, C. S. Pattichis, M. Pantziaris, and A. N. Nicolaides, "Texture-based classification of atherosclerotic carotid plaques," *IEEE Trans. Med. Imag.*, vol. 22, no. 7, pp. 902–912, Jul. 2003.

[10] N. N. Tsiaparas, S. Golemati, I. Andreadis, J. S. Stoitsis, I. Valavanis, and K. S. Nikita, "Comparison of multiresolution features for texture classification of carotid atherosclerosis from B-mode ultrasound," *IEEE Trans. Inf. Technol. Biomed.*, vol. 15, no. 1, pp. 130–137, Jan. 2011.

[11] S. Mougiakakou, S. Golemati, I. Gousias, A. N. Nicolaides, and K. S. Nikita, "Computer-aided diagnosis of carotid atherosclerosis based on ultrasound image statistics, Laws' texture and neural networks," *Ultrasound Med. Biol.*, vol. 33, no. 1, pp. 26–36, 2007.

[12] E. C. Kyriacou, C. S. Pattichis, M. A. Karaolis, C. P. Loizou, C. I. Christodoulou, M. S. Pattichis, S. Kakkos, and A. Nicolaides, "An integrated system for assessing stroke risk," *IEEE Eng. Med. Biol. Mag.*, vol. 26, no. 5, pp. 43–50, Sep.–Oct. 2007.

[13] E. Kyriacou, M. S. Pattichis, C. S. Pattichis, A. Mavrommatis, C. I. Christodoulou, S. Kakkos, and A. Nicolaides, "Classification of atherosclerotic carotid plaques using morphological analysis on ultrasound images," *Appl. Intell.*, vol. 30, no. 1, pp. 3–23, 2009.

[14] U. R. Acharya, S. V. Sree, M. M. R. Krishnan, F. Molinari, L. Saba, S. Y. S. Ho, A. T. Ahuja, S. C. Ho, A. Nicolaides, and J. S. Suri, "Atherosclerotic risk stratification strategy for carotid arteries using texture-based features," *Ultrasound Med. Biol.*, vol. 38, no. 6, pp. 899–915, 2012.

[15] N. N. Tsiaparas, S. Golemati, I. Andreadis, J. Stoitsis, I. Valavanis, and K. S. Nikita, "Assessment of carotid atherosclerosis from B-mode ultrasound images using directional multiscale texture features," *Meas. Sci. Technol.*, vol. 23, p. 114004, 2012. Available: http://iopscience.iop.org/0957-0233/23/11/114004/

[16] U. R. Acharya, O. Faust, S. V. Sree, F. Molinari, L. Saba, and A. Nicolaides, "An accurate and generalised approach to plaque characterization in 346 carotid US scans," *IEEE Trans. Instrum. Meas.*, vol. 61, no. 4, pp. 1045–1053, Apr. 2012.

[17] U. R. Acharya, O. Faust, V. Sree S., A. P. Alvin, G. Krishnamurthi, J. C. Seabra, J. Sanches, and J. S. Suri, "Understanding symptomatology of atherosclerotic plaque by image-based tissue characterization," *Comput. Methods Programs Biomed.*, vol. 110, no. 1, pp. 66–75, 2013.

[18] M. G. Tsipouras, T. P. Exarchos, D. I. Fotiadis, A. P. Kotsia, K. V. Naka, and L. K. Michalis, "Automated diagnosis of coronary artery disease based on data mining and fuzzy modeling," *IEEE Trans. Inf. Technol. Biomed.*, vol. 12, no. 4, pp. 447–458, Jul. 2008.

[19] C. Zhou, H. P. Chan, B. Sahiner, L. M. Hadjiiski, A. Chughtai, S. Patel, J. Wei, P. N. Cascade, and E. A. Kazerooni, "Computer-aided detection of pulmonary embolism in computed tomographic pulmonary angiography (CTPA): Performance evaluation with independent data sets," *Med. Phys.*, vol. 36, no. 8, pp. 3385–3396, 2009.

[20] M. McCormick, T. Varghese, X. Wang, C. Mitchell, M. A. Kliewer, and R. J. Dempsey, "Methods for robust in vivo strain estimation in the carotid artery," *Phys. Med. Biol.*, vol. 57, no. 22, pp. 7329–7353, 2012.

[21] A. Gastounioti, S. Golemati, J. S. Stoitsis, and K. S. Nikita, "Adaptive block matching methods for carotid artery wall motion estimation from B-mode ultrasound: In silico evaluation & *in vivo* application," *Phys. Med. Biol.*, vol. 58, no. 24, pp. 8647–8661, 2013.

[22] A. Gastounioti, V. Kolias, S. Golemati, N. N. Tsiaparas, A. Matsakou, J. S. Stoitsis, N. P. E. Kadoglou, C. Gkekas, J. D. Kakisis, C. D. Liapis, P. Karakitsos, I. Sarafis, P. Angelidis, and K. S. Nikita, "CAROTID—A web-based platform for optimal personalized management of atherosclerotic patients," *Comput. Method Programs Biomed.*, vol. 114, no. 2, pp. 183–193, 2014.

[23] I. M. Graf, F. H. B. M. Schreuder, J. M. Hameleers, W. H. Mess, R. S. Reneman, and A. P. G. Hoeks, "Wall irregularity rather than intima-media thickness is associated with nearby atherosclerosis," *Ultrasound Med. Biol.*, vol. 35, no. 6, pp. 955–961, 2009.

[24] A. Gastounioti, S. Golemati, and K. S. Nikita, "Computerized analysis of ultrasound images: Potential associations between texture and motion properties of the diseased arterial wall," presented at the IEEE Int. Ultrasonics Symp., Dresden, Germany, 2012.

[25] A. Gastounioti, S. Golemati, J. Stoitsis, and K. S. Nikita, "Comparison of Kalman-filter-based approaches for block matching in arterial wall motion analysis from B-mode ultrasound," *Meas. Sci. Technol.*, vol. 22, no. 11, p. 9, 2011. Available: http://iopscience.iop.org/0957-0233/22/11/114008

[26] S. Golemati, J. S. Stoitsis, A. Gastounioti, A. C. Dimopoulos, V. Koropouli, and K. S. Nikita, "Comparison of block matching and differential methods for motion analysis of the carotid artery wall from ultrasound images," *IEEE Trans. Inf. Technol. Biomed.*, vol. 16, no. 5, pp. 852–858, Sep. 2012.

[27] J. C. Burges, "A tutorial on support vector machines for pattern recognition," *Data Min. Knowl. Disc.*, vol. 2, no. 2, pp. 1–43, 1998.

[28] L. Shutao, J. T. Kwok, H. Zhu, and Y. Wang, "Texture classification using support vector machines," *Pattern Recog.*, vol. 36, no. 12, pp. 2883–2893, 2003.

[29] D. F. Specht, "Probabilistic neural networks," *J Neural Netw.*, vol. 3, pp. 109–118, 1990.

[30] J. Han, M. Kamber, and J. Pei, *Data Mining: Concepts and Techniques*. 3rd ed. Waltham, MA, USA: Elsevier, 2012.

[31] J. R. Quinlan, "Induction of decision trees," *Machine Learning*. vol. 1, Norwell, MA, USA: Kluwer, 1986, no. 1, pp. 81–106.

[32] R. O. Duda, P. E. Hart, and D. H. Stork, *Pattern Classification*. New York, NY, USA: Wiley, 2000.

[33] P. Refaeilzadeh, L. Tang, and H. Liu, "Cross-Validation," *Encyclopedia of Database Systems*. New York, NY, USA: Springer, 2009, pp. 532–538.
[34] T. Fawcett, "ROC graphs: Notes and practical considerations for data mining researchers," HP Laboratories, Palo Alto, CA, USA, Tech. Rep. HPL-2003–2004, 2003.
[35] G. Zahnd, L. Boussel, A. Marion, M. Durand, P. Moulin, A. Serusclat, and D. Vray, "Measurement of two-dimensional movement parameters of the carotid artery wall for early detection of arteriosclerosis: A preliminary clinical study," *Ultrasound Med. Biol.*, vol. 37, no. 9, pp. 1421–1429, 2011.
[36] T. Passerini, L. M. Sangalli, S. Vantini, M. Piccinelli, S. Bacigaluppi, L. Antiga, E. Boccardi, P. Secchi, and A. Veneziani, "An integrated statistical investigation of internal carotid arteries of patients affected by cerebral aneurysms," *Cardiovascular Eng. Technol.*, vol. 3, no. 1, pp. 26–40, 2012.
[37] L. M. Sangalli, P. Secchi, S. Vantini, and A. Veneziani, "A case study in exploratory functional data analysis: Geometrical features of the internal carotid artery," *J. Am. Statist. Assoc.*, vol. 104, no. 485, pp. 37–48, 2009.

Aimilia Gastounioti (M'10) received the Diploma degree in electrical and computer engineering from the National Technical University of Athens (NTUA), Athens, Greece, in 2009, where she is currently working toward the Ph.D. degree in the Biomedical Simulations and Imaging Laboratory, NTUA.

She has (co-)authored 17 papers in scientific journals and international conferences and one book chapter. She has also worked as a Researcher in two National and two European R&D projects on biomedical engineering. Her current research interests include medical image processing and analysis, and machine learning toward computer-aided clinical diagnosis.

Since 2012, Ms. Gastounioti has been a Scientific Reviewer of the IEEE JOURNAL OF BIOMEDICAL AND HEALTH INFORMATICS, the Wiley-*Scanning*, and the Elsevier-*Ultrasonics*, as well as in various international scientific conferences. She has participated at the organizing committees of three international scientific conferences. She is a Member of the Technical Chamber of Greece.

Stavros Makrodimitris was born in Athens, Greece, in 1991. He received the Diploma degree in electrical and computer engineering from the National Technical University of Athens (NTUA), Athens, Greece, in 2013. He is currently working toward the Master's degree program on bioinformatics at the Delft University of Technology, Delft, The Netherlands, and Leiden University, Leiden, The Netherlands.

Mr. Makrodimitris is a Member of the Technical Chamber of Greece.

Spyretta Golemati (M'97) received the Diploma degree in mechanical engineering from the National Technical University of Athens (NTUA), Athens, Greece, in 1994, and the M.Sc. and Ph.D. degrees in bioengineering from Imperial College of Science, Technology, and Medicine, University of London, London, U.K., in 1995 and 2000, respectively.

She was a Postdoctoral Fellow in the Department of Electrical and Computer Engineering, NTUA. She is currently a Lecturer in Department of Biomedical Engineering, National Kapodistrian University of Athens, Athens. Her research interests include ultrasound imaging and signal analysis, arterial biomechanics, and respiratory mechanics. She has coauthored 26 papers in international scientific journals, seven book chapters, and 40 papers in international conference proceedings. She is an Associate Editor in Elsevier's *Ultrasonics journal*.

Nikolaos P. E. Kadoglou received the Diploma degree from the Medical School, Aristotle University of Thessaloniki, Thessaloniki, Greece, in 2000, and the Master of Science degree in exercise and health from the Aristotle University of Thessaloniki, in 2004. He received the Ph.D. degree from the Medical School, University of Athens, Athens, Greece, in 2008, and the second Ph.D. degree from the Aristotle University of Thessaloniki, in 2013, and the Postdoctoral degree from the Biomedical Research Foundation Academy of Athens, Athens, Greece, in 2013.

He completed the specialty training in Cardiology in 2013 and since then he has been working as an Attending Cardiologist in the Department of Vascular Surgery, Attikon University Hospital of Athens, Athens, Greece, and in private office. He has (co-)authored 55 papers in scientific journals with impact factor and numerous citations (725, h-index 14). He has performed more than 100 oral announcements and posters presentations in international and national congresses and has awarded three grants for postgraduate studies. He has participated as a Principal Investigator in eight international research projects.

Christos D. Liapis received the Diploma degree, in 1972 and the Ph.D. degree, in 1982 from the Medical School of Athens, Athens, Greece.

He is currently the Head of the Department of Vascular Surgery, Athens University Medical School, Athens, Greece, and is involved in several ongoing national and international studies. His 35-year career in vascular surgery spans major academic and clinical posts from the U.S. to Europe. During his term as the Secretary-General of the UEMS Division and Board of Vascular Surgery from 1999 to 2004, he played a key role in the Board Examinations, European Vascular CME and the establishment of Vascular Surgery as an independent Specialty Section in Europe. He served as the President of the European Society of Vascular Surgery from 2004 to 2005. He is currently the President of the International Society for Vascular Surgeons. He has written more than 300 articles and a number of books.

Konstantina S. Nikita (M'96–SM'00) received the Diploma degree in electrical engineering and the Ph.D. degree from the National Technical University of Athens (NTUA), Athens, Greece, and the M.D. degree from the Medical School, University of Athens, Athens, Greece.

Since 2005, she has been a Professor at the School of Electrical and Computer Engineering, NTUA. She has also served as the Deputy Head of the School of Electrical and Computer Engineering of the NTUA. She has authored or co-authored 176 papers in refereed international journals and chapters in books, and more than 300 papers in international conference proceedings. She is the Editor of four books in English, and author of two books in Greek. She holds two patents. She has been the Technical Manager of several European and National R&D projects. Her current research interests include biological effects and medical applications of radiofrequency electromagnetic fields, biomedical telemetry, biomedical signal and image processing and analysis, simulation of physiological systems, and biomedical informatics.

Dr. Nikita has been the Honorary Chair/Chair of the program/organizing committee of several international conferences and she has served as the Keynote/Invited Speaker at international conferences, symposia and workshops organized by NATO, WHO, ICNIRP, IEEE, URSI, COMCON, PIERS, etc. She has been the advisor of 22 completed Ph.D. theses, several of which have received various awards.

She is an Associate Editor of the IEEE TRANSACTIONS ON BIOMEDICAL ENGINEERING, the IEEE JOURNAL OF BIOMEDICAL AND HEALTH INFORMATICS, the Wiley-*Bioelectromagnetics*, the *Journal of Medical and Biological Engineering and Computing*, and a Guest Editor of several international journals. She has received various honors/awards, among which, the Bodossakis Foundation Academic Prize (2003) for exceptional achievements in "Theory and Applications of Information Technology in Medicine." She has been a member of the Board of Directors of the Atomic Energy Commission, of the Hellenic National Academic Recognition and Information Center, and of the Hellenic National Council of Research and Technology. She is a member of the Hellenic National Ethics Committee, a Founding Fellow of the European Association of Medical and Biological Engineering and Science, a member of the Technical Chamber of Greece and of the Athens Medical Association. She is also the Founding Chair and the Ambassador of the IEEE-Engineering in Medicine and Biology Society, Greece chapter and the Vice Chair of the IEEE Greece Section.